J. Phys. Chem. A **2000,** *104,* 9605−9612

Ab Initio Investigation of the Temporary Anion States of Perfluoroethane

M. F. Falcetta*,†

Department of Chemistry, Anderson University, Anderson, Indiana 46012

Y. Choi

United States Environmental Protection Agency, 2565 Plymouth Road, Ann Arbor, Michigan 48105

K. D. Jordan*,‡

Department of Chemistry and Center for Molecular and Materials Simulations, University of Pittsburgh, Pittsburgh, Pennsylvania 15260

Received: May 12, 2000; In Final Form: August 15, 2000

The stabilization method is used to characterize the temporary anion states of C_2F_6. Based on the theoretical results, we assign the lowest-energy feature in the electron transmission spectrum of C_2F_6 to the ^2E_u ground-state anion and the second feature to overlapping 1^2A_u, 1^2A_{1g}, 2^2A_u, and 1^2E_g anion states. It is also proposed that the bimodal kinetic energy distribution of the F^- ions produced in the dissociative attachment of near 5 eV electrons on C_2F_6 is due to the Jahn−Teller effect.

I. Introduction

Anion states that lie energetically above the ground state of a neutral molecule are unbound with respect to electron autoionization. These temporary anions (or resonances) can be characterized by means of electron transmission spectroscopy (ETS)[1,2,3] and other electron impact techniques. The key data provided by ETS measurements are the vertical electron attachment energies (VAEs), that is, the energies of the anion states relative to that of the neutral molecule, at the equilibrium geometry of the latter.

Unsaturated molecules such as ethylene, benzene, and formaldehyde have relatively low energy temporary anion states resulting from electron capture into unfilled π^* orbitals. In contrast, acyclic saturated molecules containing only hydrogen and second-row elements (C, O, etc.) generally do not possess low-lying (VAE $\leq$ 6 eV) temporary anion states.[3] The perfluoro-*n*-alkanes (hereafter referred to simply as the perfluoroalkanes) represent an important exception to this general rule. ET measurements[4] show that the lowest VAE of the perfluoroalkanes decreases from 4.6 eV in *n*-C_2F_6 to 1.2 eV in *n*-C_6F_{14}. Evidence for the existence of low-lying anion states in the perfluoroalkanes is also provided through dissociative attachment (DA) measurements[5] and total scattering cross-section measurements.[6] However, the assignment of the anion states of the perfluoroalkanes is a subject of considerable debate. In this work, we examine theoretically the temporary anion states of C_2F_6 and reinterpret the experimental results for this system.

For the D_{3d} staggered global potential energy minima, simple molecular orbital considerations lead one to expect both C_2H_6 and C_2F_6 to have five valence-type unfilled MOs, two of a_{2u} symmetry and one each of e_u, e_g, and a_{1g} symmetry. However, the electron transmission spectrum of C_2H_6 fails to provide evidence of low-lying anion states, a very broad feature, due to one or more overlapping anion states, centered near 7.5 eV, is evident in electron-impact vibrational excitation cross sections.[7] In contrast, the electron transmission spectrum of C_2F_6 displays two broad peaks centered at 4.6 and 8.9 eV (with widths of 1.5 and 3.0 eV, respectively) suggesting that either some of the anion states of C_2F_6 are not observed or that one or both peaks are due to overlapping anion states.[4] The reasons for the greater prominence of valence-type anion states in C_2F_6 as compared to C_2H_6 will be discussed later in the paper.

The first attempt to assign the temporary anion states of C_2F_6 and larger perfluoroalkanes was by Ishii et al.[4] who made use of Koopmans' theorem (KT)[8] in conjunction with the STO-3G basis set.[9] In the KT approach, the VAEs are associated with the energies of the unfilled MOs obtained from Hartree−Fock calculations on the neutral molecule. The KT/STO-3G calculations predicted that the ground-state anion of C_2F_6 results from electron capture into an e_u orbital. However, it is by no means certain that such a crude approach, neglecting relaxation and correlation effects and employing a minimal basis set, reliably predicts the relative energies of the anion states. In fact, Moore and co-workers[6] have noted that the energies of the unfilled MOs of the perfluoroalkanes are extremely sensitive to the atomic basis set employed, and have questioned the usefulness of MO calculations for assigning the anion states. These authors have also found that the peaks in the total electron scattering cross section for C_2F_6 fall close in energy to the features observed in the ET spectrum, and they concluded that the lowest-energy feature is due to electron capture into an a_{2u} orbital. Takagi et al. measured electron-impact vibrational excitation cross sections for C_2F_6 and interpreted their results in terms of an $^2A_{2u}$ assignment for the 4.6 eV feature.[10] Weik and Illenberger[5] observed a break in the kinetic energy distribution of the F^- ions produced in dissociative attachment (DA) measurements on C_2F_6 (for incident electron energies between

---

* Author to whom correspondence should be addressed. E-mail: falcetta_michael@roberts.edu.

† Present address: Division of Natural Sciences and Mathematics, Roberts Wesleyan College, 2301 Westside Drive, Rochester, NY 14624-1997.

‡ E-mail: ken@theory.chem.pitt.edu.

10.1021/jp001782l CCC: \$19.00

4 and 5 eV). On this basis, they suggested that the lowest-energy feature observed in the electron transmission derives from both $^2A_{2u}$ and ^2E_u anion states. Hence three different assignments—^2E_u alone, ^2A_u alone, and both ^2E_u and ^2A_u states—have been made for the 4.6 eV electron capture process C_2F_6. The assignment of the state or states involved in the 8.9 eV electron capture process is equally uncertain. The goal of the present theoretical investigation is to resolve the controversies concerning the assignments of the anion states of C_2F_6. To this end the VAEs of C_2F_6 have been calculated using methods that have been explicitly designed for treating resonances. Before describing the details of the calculations, we first address some misconceptions about the use of such MO-based procedures for describing temporary anion states.

II. Applications of MO Methods to Temporary Anion States

It is a commonly held view that the KT procedure is less viable for anion states than cation states. Two factors have contributed to this view. First, for systems with only temporary anion states, all virtual orbitals obtained from Hartree–Fock calculations on the neutral atom or molecule appear at positive energies. In general, these unbound virtual orbitals can be divided into two groups: (1) those that correspond to temporary anion states in a KT sense, and (2) those that correspond to approximations to continuum solutions, hereafter referred to as discretized continuum (DC) solutions.[11,12] Moreover, there may be large mixing between the two types of virtual orbitals. Second, even assuming "correct" virtual orbitals can be identified, relaxation and electron correlation contributions to VAEs tend to be of the same sign and, as a result, KT estimates of the VAEs would be expected to be appreciably (2–4 eV) higher than those determined experimentally. It is now well established, if not widely appreciated, that the first problem can be solved by use of the stabilization method,[13] which allows one not only to identify which virtual orbitals correspond to temporary anion states in a KT sense, but also to obtain well converged energies for those orbitals as the basis set is enlarged. In addition, it has been demonstrated in several studies that the KT procedure, when combined with stabilization, is generally very successful at predicting the relative VAEs of isolated molecules as well as the trends in the VAEs along series of closely related molecules.[11,12,14,15]

When using a minimal basis set, all virtual orbitals are necessarily localized in the molecular region and thus appear valence-like. There are two serious limitations of such calculations. First, they may erroneously lead one to expect there to be well-defined valence-type anion states, when, in fact, such states are not observed experimentally. Second, for molecules that do possess valence-type temporary anion states, small basis set calculations may not be able to account even qualitatively for the trends in the relative energies of various anion states.

As one expands the basis set to provide a better description of the temporary anion states, the DC solutions fall lower and lower in energy. For unsaturated molecules Hartree–Fock calculations using modest sized "double-ζ" split-valence basis sets, such as 3-21G[16] or 6-31G(d),[17] generally place the unfilled orbitals that correspond to π^* anion states appreciably below the lowest-energy DC levels.[18] It is for this reason that MO calculations using the 3-21G and 6-31G(d) basis sets have proven so useful in interpreting the electron transmission spectra of unsaturated molecules.[3,14,19] However, for saturated molecules the lowest-energy DC levels with these basis sets may fall energetically close or below the MOs corresponding to the anion states. Finally, with the inclusion of diffuse functions in the basis set, e.g., the "+" functions in the 6-31+G basis set,[20] the lowest-energy DC solutions generally fall below the orbitals that correspond to the valence-type anion states even for unsaturated molecules. With these and larger basis sets, it is essential to combine the MO calculations with the stabilization[13] or other methods for determining the orbitals (and associated energies) that correspond to the temporary anion states in the KT sense. Hereafter, these will be referred to as stabilized Koopmans' theorem (SKT) levels.[12]

The identification of SKT levels is of import beyond the assignment of anion states in ET and other electron impact spectroscopies. In particular, there appears to be a close correspondence between the existence of unfilled MOs that correspond to anion states in a KT sense and the existence of well-defined valence-like transitions in the optical spectra of a molecule.[21] For example, although the optical spectra of the perfluoroalkanes display prominent valence transitions, those of the corresponding alkanes do not.[22] The failure to observe valence excited states in the *n*-alkanes (as well as in molecules such as H_2O and NH_3) is due to strong valence/Rydberg mixing. In the words of Robin, the excited valence states have "dissolved in the Rydberg sea".[23] Similarly, the failure to observe an expected anion state in an ET spectrum or SKT calculation can be understood in terms of large couplings to the electron autoionization continuum causing the anion state to be so broad that it is difficult or impossible to detect in a total scattering cross section such as that measured using ETS. Molecules for which the expected unfilled valence-type MOs are so strongly coupled to the autoionization continuum that they do not form readily identifiable temporary anion states, are precisely those for which valence/Rydberg mixing causes the "expected" valence-like excited states to "disappear".

III. Computational Methods

In this work the stabilization method will be the main approach for characterizing the temporary anion states. This approach exploits the fact that, in contrast to the DC solutions, the wave functions corresponding to the temporary anion states have their amplitude localized in the molecular region. As a consequence, varying the radial extent of the most diffuse basis functions affects the energies of the DC solutions much more than it affects the energies of the temporary anion solutions. In the SKT method, the most diffuse functions in the basis set are systematically scaled and the virtual orbital energies are plotted as a function of the scaling factor, α, yielding a stabilization graph.[13] In cases where the SKT level of interest is well separated from DC levels (of the same symmetry) over the range of α values examined, the energy of the SKT level can be estimated simply from inspection of the stabilization graph. With sufficiently flexible basis sets, the SKT levels will experience avoided crossings with one or more DC levels as α is varied. The energies of the SKT levels can then be estimated by graphically constructing the corresponding diabatic levels. However, when there are several DC solutions in the same energy region as the SKT solution, it becomes difficult to obtain a reliable estimate of the SKT energy from the stabilization graph, and instead, a density-of-states (DOS) method recently introduced by Taylor and co-workers[24] is used for this purpose. The implementation of the DOS method is described in the Appendix.

In distinguishing the SKT and DC levels of the molecular system, it is useful to solve the one-electron Schrodinger equation for a "free" electron as described by the molecular

TABLE 1: Energies (eV) of the Unfilled Orbitals of C_2F_6[a,b]

symmetry	STO-3G	3-21G	6-311G(d)[c]	6-311+G(d)[c]	SKT[d]
e_u	$\underline{13.2}$ (24.5)	$\underline{7.2}$, 23.4 (10.9)	$\underline{7.1}$, 15.9 (7.6, 18.1)	2.7, $\underline{6.8}$, $\underline{9.4}$, 10.3, 11.5, 15.8 (2.2, 7.3, 8.5, 9.4, 14.4, 19.5)	7.4
a_{1g}	$\underline{16.8}$ (9.4, 30.5)	$\underline{10.8}$, 25.9 (5.6, 15.0)	$\underline{9.4}$, 14.7 (3.7, 11.1, 17.2)	2.2, 3.7, $\underline{9.7}$, $\underline{10.3}$, $\underline{11.6}$, 13.2 (1.1, 3.3, 5.2, 9.1, 11.0, 14.9, 19.3)	11.4
a_{2u}	$\underline{15.6}$, $\underline{16.8}$ (14.7, 38.6)	$\underline{10.6}$, $\underline{11.2}$, 22.7 (8.6, 22.4)	$\underline{9.8}$, $\underline{11.4}$, $\underline{14.7}$ (6.1, 16.0,19.0)	2.5, 5.2, 8.9, $\underline{10.4}$, $\underline{11.1}$, $\underline{13.0}$, 16.1 (2.0, 4.9, 7.2, 9.5, 13.1, 17.9)	10.9, 11.6
e_g	$\underline{18.6}$ (26.7)	$\underline{13.1}$, 26.8 (14.5)	$\underline{12.4}$, 17.7 (10.4, 16.7)	3.6, 7.4, $\underline{11.4}$, $\underline{12.4}$, $\underline{13.2}$, 15.0 (3.3, 6.4, 9.2, 12.0,13.6, 20.2)	12.3

[a] Levels that correspond to anion states in a KT sense are underlined. [b] The energies of the 1e-DC solutions are given in parentheses. [c] Orbital energies below 19 eV. [d] Obtained with the 6-311+G(d) basis set, scaling the two most diffuse SP functions on the C and F atoms.

basis set but ignoring the other electrons and setting all nuclear charges equal to zero.[11,12] The resulting one-electron discretized continuum (1e-DC) levels generally lie lower in energy than the DC levels obtained from the HF calculations on the actual molecule. This reflects the destabilization of the DC levels due to orthogonality to the occupied orbitals of the same symmetry and to "excluded volume" effects. Comparison of the energies of the unfilled orbitals from Hartree−Fock calculations on the molecule of interest with those of the 1e-DC solutions may enable one to determine which low-lying unfilled orbitals correspond to anion states in the KT sense even without exponent scaling.

The stabilization and DOS methods for identifying resonances can also be used in conjunction with methods that include relaxation and correlation contributions to the VAEs, and in this work, the energies of the anion levels will also be estimated using the S-ΔMP2 method. This approach combines the stabilization method with a modified ΔMP2 method. As traditionally used, the ΔMP2 method would simply entail carrying out separate MP2 calculations on the neutral and anionic molecule and taking the difference between these two energies. However, in extending this approach to temporary anion states, it is essential to allow for the possibility of low-lying DC solutions in the same energy range or energetically below the anion of interest. Here we accomplish this by using the complete-active space MP2 (CASPT2) procedure[25] to describe the $N + 1$ electron system, while retaining the single-reference MP2 procedure for the ground state of the N-electron neutral molecule. The reference space for the CASPT2 calculations is chosen to ensure that the anion state of interest is encompassed regardless of whether there are lower-lying DC levels of the same symmetry. In addition, the CASPT2 calculations allow for the extraction of multiple eigenvalues, which is essential for application of the stabilization method.

In our application of the S-ΔMP2 method to C_2F_6, the 6-311+G(d) basis set[26] was employed. (Justification for the use of this basis set is provided below.) The exponents of the two most diffuse sets of sp functions on each atom were simultaneously scaled. The reference spaces contained 12 to 15 configurations,[27] depending on the symmetry of the anion state being considered. The reference spaces were chosen to ensure that, over the range of α employed, all orbitals that might mix with the resonance (in a KT approach) are included. For the $N + 1$ electron states, the CASPT2 calculations were preceded by complete-active-space SCF (CASSCF) calculations in which the MOs occupied in the HF wave function for the neutral molecule were kept inactive, i.e., restricted to double occupancy but allowed to relax, and the active "excess" electron was allowed to occupy any of the normally empty MOs of the symmetry of interest. The CASPT2 calculations were carried out using the CASSCF wave functions as the reference functions. One root was extracted for each configuration included in the reference space. The MOs that correspond to the 1s AOs were kept frozen in both the MP2 and CASPT2 calculations.

Unless noted otherwise, all theoretical results are reported at the geometry of the neutral molecule, which was optimized at the MP2/6-31G(d) level and assuming D_{3d} symmetry. The calculations were performed using the Gaussian 98[28] and MOLCAS 3.2[29] programs.

IV. Results and Discussion

Choice of Basis Sets. The first step in carrying out stabilization calculations is to determine suitable basis sets. To this end, stabilization calculations at the KT level were carried out on C_2F_6 using the 6-31+G(d), 6-311+G(d), and several larger basis sets. These calculations revealed that the 6-311+G(d) basis set is sufficiently flexible to describe the valence-like SKT levels of C_2F_6. In general, the inclusion of relaxation and correlation contributions necessitates use of more flexible basis sets than do KT calculations. Therefore it is somewhat surprising that the 6-311+G(d) basis set also appears to be suitable for characterizing the anion states of perfluoroalkanes at the S-ΔMP2 level of theory. This was established by calculating the vertical attachment energy of CF_4 (for forming the $^2T_2$ anion) at the S-ΔMP2 level and using three different basis sets: 6-311+G(d), 6-311+G(3d), and 6-311+G(3d,p). The CF_4 molecule was chosen in place of C_2F_6, due to the smaller computational demands. The 6-311+G(3d) basis set was formed from the 6-311+G(d) by replacing the single d function with the three d functions from the aug-cc-pVTZ basis set.[30] The 6-311+G(3d,p) basis set was constructed by also adding on all atoms single primitive p Gaussian-type functions with exponents three times smaller than those of the most diffuse p functions in the 6-311+G(d) basis set. The S-ΔMP2 calculations with the 6-311+G(d), 6-311+G(3d), and 6-311+G(3d,p) basis sets gave VAEs of 7.7, 7.4, and 7.5 eV, respectively, as compared with the experimental value of 7.3 eV. These results indicate that, even in calculations including correlation and relaxation effects, the $^2T_2$ anion of CF_4 is well described by the 6-311+G(d) basis set. Accordingly, this basis set was adopted for the S-ΔMP2 calculations on C_2F_6. In the SKT approximation, the VAE of CF_4 (for formation of the $^2T_2$ anion) is 11.1 eV, compared with the S-ΔMP2 value of 7.7 eV (with the 6-311+G(d) basis set). Thus, relaxation and correlation corrections lower the energy of the anion state relative to that of the neutral molecule by about 3.4 eV.

KT and SKT Results. Table 1 lists for C_2F_6 the energies of the virtual MOs obtained from HF calculations using each of the STO-3G, 3-21G, 6-311G(d), and 6-311+G(d) basis sets. The STO-3G and 3-21G basis sets have been included in order to determine whether the low-lying virtual MOs obtained using such small basis sets adequately reproduce the relative energies

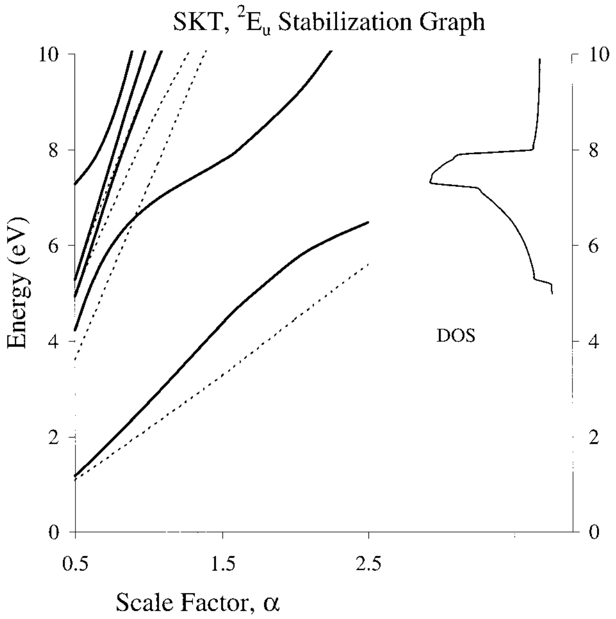

Figure 1. SKT stabilization graph for the e_u symmetry block of C_2F_6, obtained with the 6-311+G(d) basis set. Virtual orbital energies are given by the solid curves, while the 1e-DC levels are given by the dashed curves. The inset shows the density of states (DOS), with the vertical axis being the same as that of the stabilization graph and the horizontal axis in arbitrary units.

of the SKT levels as obtained from stabilization calculations. The energies of the 1e-DC solutions obtained with each of these basis sets as well as the SKT energies obtained using the 6-311+G(d) basis set are also reported. We consider in detail the results for e_u symmetry; the analysis of the results in the other symmetry blocks is analogous.

For the STO-3G basis set, only a single virtual orbital of e_u symmetry is obtained, and, although very high in energy, this orbital corresponds to the ^2E_u anion state since it lies more than 12 eV below the lowest e_u 1e-DC level. With the 3-21G basis set, the lowest-energy unfilled orbital of e_u symmetry falls at 7.2 eV. Once again, this is attributed to the temporary anion state because the lowest-energy e_u 1e-DC level calculated with this basis set lies higher in energy (at 10.9 eV). With the 6-311G(d) basis set, the lowest-energy unfilled orbital lies at 7.1 eV, and the lowest-energy 1e-DC level lies at 7.6 eV. While the lowest-energy unfilled orbital of e_u symmetry can still be associated with the temporary anion the decrease in the energy of the 1e-DC level with increasing diffuseness of the basis set is apparent. The situation is more complicated with the 6-311+G(d) basis set, for which there are three unfilled MOs and four 1e-DC levels of e_u symmetry below 10 eV. There are fewer unfilled MOs than 1e-DC solutions below 10 eV because the third and fourth 1e-DC levels are "pushed" well above 10 eV in the calculations on the molecule. The stabilization graph shown in Figure 1 shows that for $\alpha \approx 1$ the valence-type character is distributed between the 6.8 eV and higher-lying unfilled e_u MOs. In other words, there is strong mixing between the unfilled MO that corresponds to the ^2E_u anion state and e_u symmetry DC levels. As seen from the figure, the second and fifth e_u virtual orbitals essentially define the avoided crossing. Taking the average of the energies of each of these orbitals at the appropriate edges of the avoided crossing (i.e., $\alpha = 0.9$ and 0.5 for the second and fifth e_u virtual orbitals, respectively) yields an SKT energy of 7.3 eV. It is interesting to note that the third and fourth e_u virtual orbitals traverse the avoided crossing region with slopes similar to those of the second and third 1e-DC levels. This suggests that these orbitals are DC levels with negligible coupling to the SKT level. This behavior is a fairly common occurrence in stabilization graphs for polyatomic molecules generated with large basis sets.

TABLE 2: SKT and S-ΔMP2 VAEs (eV) of C_2F_6[a]

state	SKT	adjusted SKT[b]	S-DMP2	experiment[c]
^2E_u	7.5	4.6	4.1	4.6
$^2A_{1g}$	11.4	8.5	8.0	7.0−10.0
$^2A_{2u}$	10.9, 11.6	8.0, 8.7	7.9, 8.7	7.0−10.0
^2E_g	12.3	9.4	9.5	7.0−10.0

[a] All calculated results obtained using the stabilization method with 6-311+G(d) basis set. [b] The adjusted SKT values are obtained by subtracting 2.9 eV from each SKT energy, so as to bring the lowest SKT VAE into agreement with experiment. [c] From ref 4.

In the case of such complicated stabilization graphs, the DOS calculated using the method of Taylor and co-workers[24] can be useful in determining the SKT energy more precisely. The DOS, displayed in the inset on the right side of Figure 1, displays a maximum centered near 7.4 eV, in close agreement with the energy of the SKT level determined from inspection of the stabilization graph.

The stabilization graphs for the unfilled orbitals of the other symmetries have been analyzed in a similar fashion and the results are summarized in Table 1. The energies for the remaining SKT levels are as follows: a_{2u} (10.9 and 11.6 eV), e_g (12.3 eV), and a_{1g} (11.4 eV). Allowing for the appreciable line widths in the electron transmission spectrum, these results lead us to assign the lowest-energy feature, observed at 4.6 eV, to the ^2E_u anion and the higher-lying feature at 8.9 eV to the other four anion states. This assignment assumes that the SKT approximation places the various anion states about 3 eV too high in energy. The S-ΔMP2 calculations, discussed below, show that this is indeed the case. Note that the general picture derived from the stabilization calculations, with the ground-state anion being ^2E_u and being separated by about 4 eV from a group of closely spaced anion states, is consistent with KT results for the STO-3G and 3-21G basis sets. As expected, the DC-like levels are sufficiently high with these basis sets that the simple KT approximation fares quite well at predicting the relative energies of the various anion states. However, it is apparent that with the more flexible basis set, mixing between the orbitals that correspond to the anon states in a KT sense and the DC levels is beginning to become problematical.

ΔMP2 Results. The stabilization graphs calculated at the S-ΔMP2 level are reported in Figures 2−5, and the S-ΔMP2 estimates of the VAEs of C_2F_6 are reported in Table 2, together with the SKT and experimental VAEs. We consider first the S-ΔMP2 stabilization graph for E_u symmetry shown in Figure 2. In the S-ΔMP2 approximation, the level that corresponds to the ^2E_u anion state lies at about 4.1 eV, which, as expected, is about 3 eV lower in energy than in the SKT approximation. A similar stabilization of the anion states upon inclusion of relaxation and correlation effects is also found in the other symmetry blocks. In general, this stabilization simplifies the analysis of the stabilization graphs as it moves the level corresponding to the anion state into an energy range less congested by DC levels.

The S-ΔMP2 stabilization graph for E_g symmetry is shown in Figure 3. Several of the eigenvalues are involved in avoided crossings at an energy of about 9.3 eV. The DOS, reported as an inset on the right side of the figure, displays a large peak at an energy of 9.3 eV and a smaller peak at 9.8 eV. In this case, we associate the energy of the anion state with the average of the two peak values, namely, 9.5 eV. Studies of model potentials

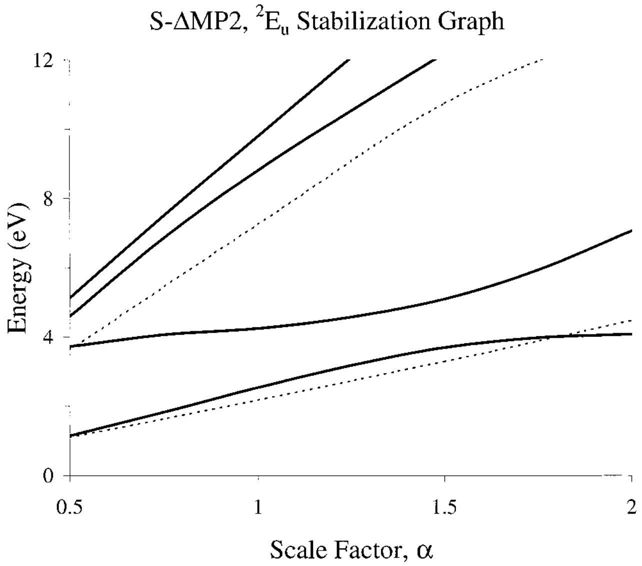

Figure 2. S-ΔMP2 stabilization graph for the ^2E_u anion state of C_2F_6, obtained with the 6-311+G(d) basis set. ΔMP2 eigenvalues are given by the solid curves, while the 1e-DC levels are given by the dashed curves.

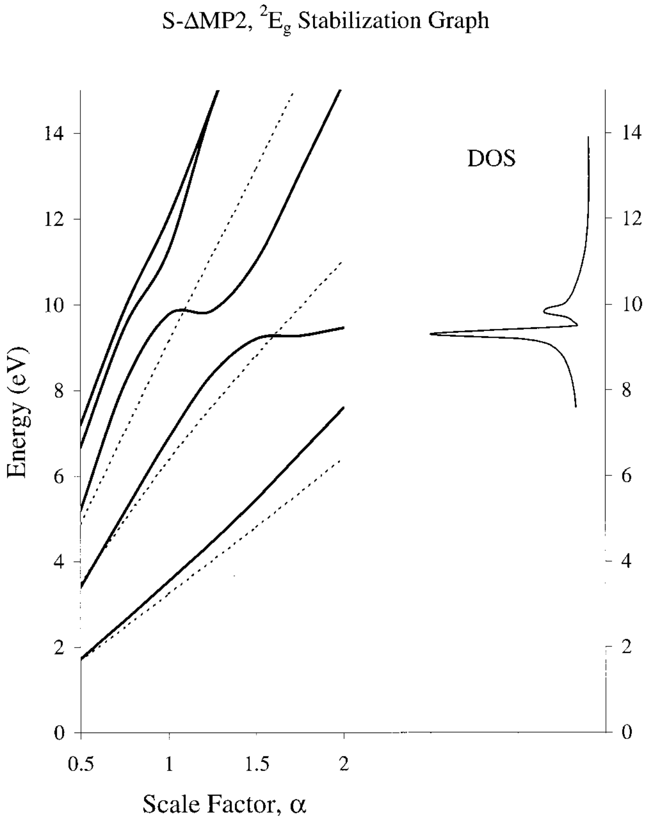

Figure 3. S-ΔMP2 stabilization graph for the ^2E_g anion state of C_2F_6, obtained with the 6-311+G(d) basis set. ΔMP2 eigenvalues are given by the solid curves, while the 1e-DC levels are given by the dashed curves. The inset shows the density of states (DOS), with the vertical axis being the same as that of the stabilization graph and the horizontal axis in arbitrary units.

reveal that, as the number of roots involved in the avoided crossings grows, the multiple peaks in the DOS overlap to give a smooth Lorentzian profile.[24]

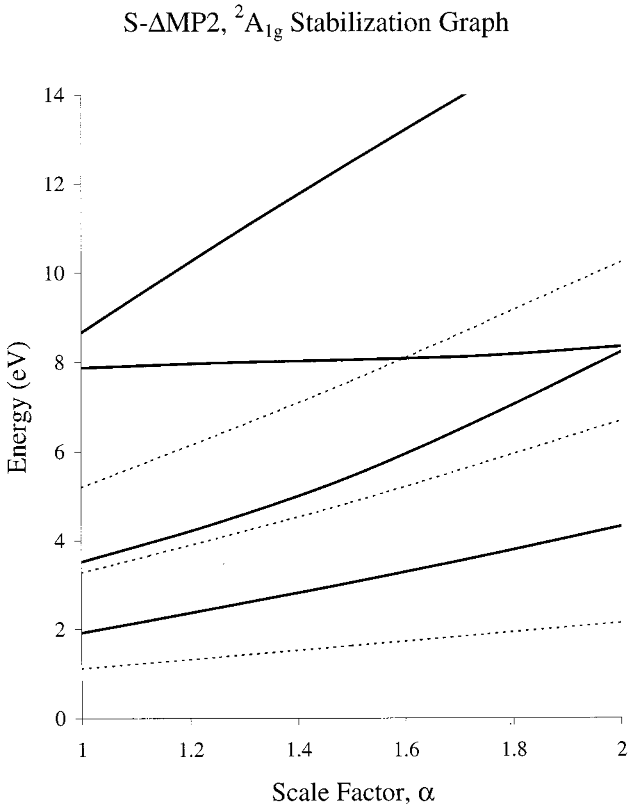

Figure 4. S-ΔMP2 stabilization graph for the $^2A_{1g}$ anion state of C_2F_6, obtained with the 6-311+G(d) basis set. ΔMP2 eigenvalues are given by the solid curves, while the 1e-DC levels are given by the dashed curves.

The S-ΔMP2 stabilization graph for the eigenvalues of A_{1g} symmetry is shown in Figure 4. In this case, the anion state is associated with the third eigenvalue near 8.0 eV, the energy of which is essentially independent of the scaling factor, for values of α between 1.0 and 1.75.

The S-ΔMP2 stabilization graph for the eigenvalues of A_{2u} symmetry is given in Figure 5. This stabilization graph is the most congested considered thus far, having two resonance solutions and three DC solutions in the energy range of interest (7−10 eV). Inspection of the stabilization graph reveals that the resonances lie close to 8.0 and 8.6 eV. This is confirmed by the DOS (see inset of Figure 5) which has peaks at 7.9 and 8.7 eV. An ambiguity in the application of the DOS method is highlighted here, namely, when two or more peaks are seen in the DOS, it may be difficult, without other corroborating evidence, to distinguish whether each peak is due to a separate resonance or whether some of the peaks are "extra" in the sense of resulting from individual resonances being involved in multiple avoided crossings. In the present case, for α > 1.75, there are three eigenvalues below 10 eV and only one 1e-DC solution, confirming the existence of two resonances.

In summary, the S-ΔMP2 calculations give a VAE of 4.1 eV for the 1^2E_u anion state and VAEs ranging from 7.9 to 9.5 eV for formation of 1^2A_{1g}, 1^2A_{2u}, 2^2A_{2u}, and 1^2E_g anion states. These predictions are in accord with the ET spectrum, which displays structure due to anion formation at 4.6 and 8.9 eV, with the latter feature having a width of about 3 eV. As expected, relaxation and correlation effects are found to lower the VAEs of the various the states by 3−4 eV. The underestimation of the VAE for forming the ^2E_u state is likely due to an imbalance in the treatment of the neutral molecule and its anion states as a consequence of the greater number of reference states employed for the MP2 calculations on the anion states.

Geometry Relaxation and Reexamination of Experimental Data. The above discussion has focused on the D_{3d} equilibrium

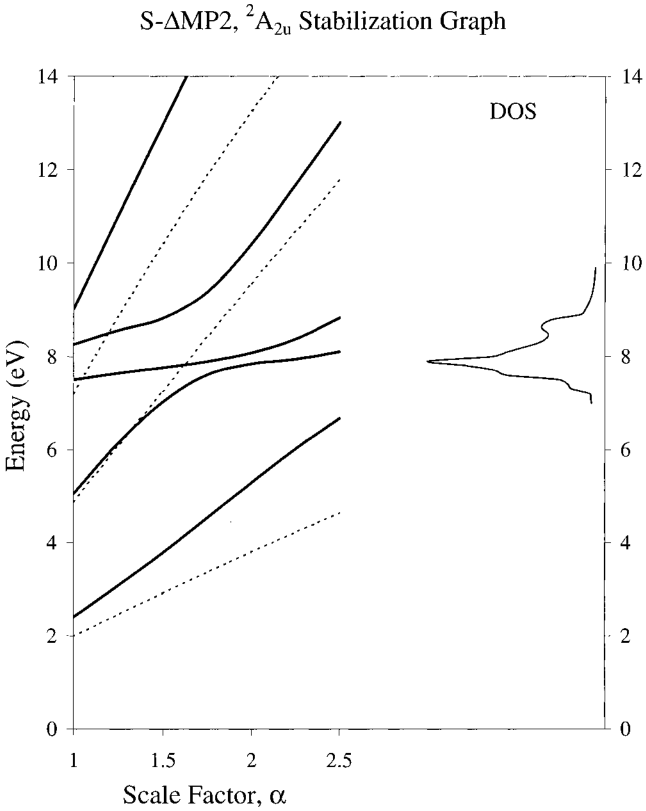

Figure 5. S-ΔMP2 stabilization graph for the $^2A_{2u}$ anion states of C_2F_6, obtained with the 6-311+G(d) basis set. ΔMP2 eigenvalues are given by the solid curves, while the 1e-DC levels are given by the dashed curves. The inset shows the density of states (DOS), with the vertical axis being the same as that of the stabilization graph and the horizontal axis in arbitrary units.

configuration of the ground state of neutral C_2F_6. We also investigated the variation of the energies of the valence-type unfilled MOs of C_2F_6 as a function of the FCCF dihedral angle. These results were based on Hartree−Fock calculations carried out on the neutral molecule and using the 6-31G(d) basis set. (Separate calculations confirm that with this basis set, the low-lying virtual MOs correspond to anion states in a KT sense rather than to DC levels.) These calculations show that the lowest-energy SKT level of C_2F_6 decreases in energy by 0.5 eV in going from the D_{3d} to the D_{3h} conformation. (This orbital is of e-type symmetry in both the D_{3d} and D_{3h} conformations.) The highest energy valence-type orbital, which is also a pair of degenerate e-type orbitals in D_{3d} and D_{3h} symmetry, increases by 0.3 eV in going from the D_{3d} to the D_{3h} conformation. The energies of the nondegenerate orbitals are essentially unchanged, although the symmetry labels do change. Thus, the basic conclusion of this study, namely that C_2F_6 has a single low-energy anion state followed by a group of four closely spaced states, holds regardless of the torsional angle.

As noted in the Introduction, Takagi et al.[10] measured the electron energy loss spectra for vibrational excitation of C_2F_6 at a scattering angle of 90° for several incident electron energies, including 4.0 and 8.5 eV. Given the widths of the features in the ET spectrum (1.5 and 3.0 eV for the first and second features, respectively), resonant scattering would be expected to dominate at these incident energies. In assigning the resonance states, Takagi et al. considered only states of A_{2u} and E_u symmetry, and made use of which vibrational levels would be expected to be excited in the neutral molecule via these intermediate anion states. On the basis of symmetry arguments, it can be shown that resonance-enhanced vibrational excitation of neutral C_2F_6 in its electronic ground state can occur in modes ν_1, ν_2, and ν_3 in the case of an intermediate $^2A_{2u}$ anion state and in modes ν_{10}, ν_{11}, and ν_{12} in the case of an intermediate ^2E_u anion state. (Other, lower frequency, symmetry-allowed modes were neglected in the analysis.) The authors noted that inclusion of ν_{11} was necessary for fitting the energy-loss spectrum for an incident energy of 8.5 eV, and on this basis assigned the higher energy resonance as the ^2E_u state. However, accurate fitting of the spectrum required excitations involving $\nu_1-\nu_3$ as well as $\nu_{10}-\nu_{12}$, which, as recognized by Takagi et al., is difficult to reconcile with the proposed assignment. Turning to the 4.0 incident energy spectrum, and assuming a $^2A_{2u}$ resonance state, Takagi et al. attempted to fit the spectrum using excitations of only modes $\nu_1-\nu_3$. While this fit accounted for most of the observed structure, inclusion of mode ν_{11} was required to account for a prominent shoulder at an energy loss of 0.065 eV, again posing a problem for the proposed assignment.

TABLE 3: Assignments of Features Found in the Electron Energy Loss Spectrum of C_2F_6 (incident electron energy of 4 eV, scattering angle of 90°)

experimental peak energy (eV)[a]	predicted peak energy (eV)[b]	mode assignment[c]
0.07	0.07	ν_{11}
0.16	0.16	ν_{10}
0.23	0.23	$\nu_{10} + \nu_{11}$
0.33	0.32	$2\nu_{10}$
0.40	0.39	$2\nu_{10} + \nu_{11}$
0.50	0.48	$3\nu_{10}$

[a] Experimental data taken from ref 10. [b] Energies of fundamental transition taken from refs 10 and 33. [c] Mode designations as listed in ref 33.

As is clear from the above discussion, the observed vibrational structure is not consistent with the assignments of the 4.6 eV resonance to the 1^2A_{2u} anion and the 8.9 eV resonance to the 1^2E_u anion. The analysis of the vibrational structure is in fact more straightforward based on our assignments of the anion states. First, the finding that a good fit of the 8.5 eV vibrational excitation spectrum requires the ν_1-ν_3 and ν_{10}-ν_{12} vibrations, is consistent with the presence of overlapping anions of A_{2u}, A_{1g} and E_g symmetries. Second, the energy-loss spectrum for incident electron energy of 4 eV can be accounted for by use of only the ν_{10}-ν_{12} modes, which is consistent with our assignment of the low-lying resonance to the ^2E_u anion state. This can be seen from Table 3, which lists the experimental peak energies determined by Takagi et al. along with our assignments, based on harmonic progressions in both ν_{10} and ν_{11}. The energies for excitation of one quanta of ν_{10} and ν_{11} are 0.16 and 0.065 eV, respectively.[31]

As also noted in the Introduction, Weik and Illenberger[5] found a break in the kinetic energy distribution of F^- ions produced in DA from C_2F_6 for incident electron energies near 5 eV, and suggested that this was due to the existence of two anion states in this energy range. In light of our results, which show that there is only one anion state near 5 eV, we propose that the bimodal kinetic energy distribution is actually due to Jahn−Teller distortions of the ^2E_u anion state. To examine this possibility, we considered distortion of $C_2F_6^-$ from D_{3d} to C_{2h} symmetry. (The Jahn−Teller effect can also cause a distortion from D_{3d} to C_i, but we did not explore this.) Under the C_{2h} distortion, the ^2E_u anion state splits into ^2A_u and ^2B_u states, with the ^2B_u anion state dropping rapidly in energy with the distortion and the ^2A_u state initially increasing in energy and then falling in energy with increasing distortion. These results are consistent with the interpretation that the bimodal distribution of the F^-

ions produced in the DA process is a consequence of the splitting of the ^2E_u state by the Jahn−Teller effect.

The geometries of both the ^2A_u and ^2B_u anion states were optimized at the MP2/6-311G(d) level of theory, and these structures were used to carry out single-point MP2 calculations using the 6-311+G(d) basis set. At its minimum energy structure, these calculations predict that the ^2B_u anion lies 1.23 eV below the neutral molecule at the same geometry. In other words, C_2F_6 is predicted to have a vertical electron detachment energy (VDE) of 1.23 eV. The ^2A_u anion state, at its optimized structure, is also bound, with VDE of 0.20 eV. Vibrational frequency calculations indicate that the ^2B_u anion is a true potential energy minimum but that the ^2A_u anion is unstable to distortion to lower symmetry.

V. Conclusions

Two pronounced features centered near 4.6 and 8.9 eV are seen in the electron transmission spectrum of C_2F_6. Based on stabilization calculations, we conclude that the lower energy feature is due to the ^2E_u ground-state anion and that the upper feature is due to the remaining four valence-type anion states. We have presented an interpretation of the energy loss spectra of Takagi et al. in accordance with these assignments and have proposed that the bimodal kinetic energy distribution observed in the F^- ions produced by dissociative attachment at incident electron energies near 5 eV is due to the splitting of the ^2E_u state by the Jahn−Teller effect. At its equilibrium C_{2h} structure, the ground-state anion lies below the neutral molecule (at the same geometry) and the vertical electron detachment energy is predicted to be about 1.23 eV. The calculated adiabatic EA is 1.57 eV.

We have established that, with the 3-21G basis set, the lowest-energy virtual orbitals obtained from HF calculations on neutral C_2F_6 can be associated with the temporary anion in the KT sense. Thus, a qualitative understanding about the SKT levels of C_2F_6 can be obtained by examining plots of the lowest-energy virtual orbitals of C_2F_6 obtained from HF/3-21G calculations. In particular, the lowest-energy (e_u) SKT level has most of its amplitude near the carbon atoms, i.e., it is largely C−C π in nature. Similarly, the e_g SKT orbital and the lower energy a_{2u} SKT orbital are largely C−C π^* and C−C σ^*, respectively. The higher energy a_{2u} SKT orbital and the a_{1g} SKT orbitals are largely CF-σ^* in nature, with low amplitude between the carbon atoms.

We now turn to the question as to why vertical electron capture occurs at an appreciably lower energy (4.6 vs 7.5 eV) in C_2F_6 than in C_2H_6. A key difference between ethane and perfluoroethane is the electronegativity of the atoms attached to the carbons. Mulliken population analyses[32] of the HF/6-31G(d) wave functions give charges on the carbon atoms of $-0.36e$ and $+1.05e$ in ethane and perfluoroethane, respectively. As noted above, the lowest-energy SKT level (e_u) of C_2F_6 has much of its charge density localized near the C atoms, and, as a result, it is strongly stabilized by the positive charges carried by these atoms. The low-lying SKT levels (and associated anion states) of the larger perfluoroalkanes can also be viewed as being a result of the positively charged carbon backbone. Interestingly, Si_2H_6 also has a relatively low-lying anion state, which in that case has been attributed to the positively charged Si atoms in the neutral molecule.[12]

Acknowledgment. This research was carried out with the support of a grant from the National Science Foundation. We acknowledge helpful discussions with Paul Burrow. The calculations were carried out on computers in the University of Pittsburgh's Center for Molecular and Materials Simulations and which were funded by IBM and NSF.

Appendix: The Density of States (DOS) Method

The general derivation of the DOS method was presented by Mandelshtam et al.[24] These authors showed that the resonant part of the DOS, as a function of energy, can be approximated as

$$<\rho\,(E)> \propto \sum_j |\,dE_j(\alpha)/d\alpha|^{-1}{}_{E_j(\alpha)=E} \qquad (A1)$$

where E_j is the energy of the jth eigenvalue of the system (in our case, the neutral molecule plus excess electron), calculated as a function of a scaling parameter, α. The bracketing of $\rho\,(E)$ indicates an averaging over the range of α considered in the stabilization graph. The sum is evaluated at the intersection of the constant energy (E) line with the E_j vs α curves, where the latter are generated by fitting the values of the jth eigenvalue evaluated at discrete values of α to spline functions. The energy, E, is then scanned over the region of interest in small (about 0.05 eV) steps. At a given E, the spline fit of E_j, is evaluated over the range of α values used to determine the value of α (if any) which causes this particular eigenvalue to match E (within a tolerance of 0.001 eV). The derivative, $dE/d\alpha$, is then evaluated at this value of α and its reciprocal is used in eq 1. This procedure is carried out for each eigenvalue in the stabilization graph. If the particular eigenvalue does not obtain a value of E in the range of α considered, it makes no contribution to the DOS.

References and Notes

(1) Sanche, L.; Schulz, G. J. *Phys. Rev. A* **1972**, *5*, 1672.
(2) Jordan, K. D.; Burrow, P. D. *Acc. Chem. Res.* **1978**, *11*, 341.
(3) Jordan, K. D.; Burrow, P. D. *Chem. Rev.* **1987**, *87*, 557.
(4) Ishii, I.; McLaren, R.; Hitchcock, A. P.; Jordan, K. D.; Choi, Y.; Robin, M. B. *Can. J. Chem.* **1988**, *66*, 2104.
(5) Weik, F.; Illenberger, E. *J. Phys. Chem.* **1995**, *99*, 1406.
(6) Sanabia, J. E.; Cooper, G. D.; Tossell, J. A.; Moore, J. H. *J. Chem. Phys.* **1998**, *108*, 389.
(7) Merz, R.; Linder, F. *J. Phys. B* **1998**, *31*, 4663.
(8) Koopmans, T. *Physica* **1934**, *1*, 104.
(9) Hehre, W. J.; Stewart, R. F.; Pople, J. A *J. Chem. Phys.* **1969**, *51*, 2675.
(10) Takagi, T.; Boesten, L.; Tanaka, H.; Dillon, M. A. *J. Phys. B* **1994**, *27*, 5389.
(11) Falcetta, M. F.; Jordan, K. D. *J. Phys. Chem.* **1990**, *94*, 5667.
(12) Falcetta, M. F.; Jordan, K. D. *Chem. Phys. Lett.* **1999**, *300*, 588.
(13) Hazi, A. U.; Taylor, H. S. *Phys. Rev. A* **1970**, *1*, 1109; Taylor, H. S.; Hazi, A. U. *Phys. Rev. A* **1976**, *14*, 2071.
(14) Burrow, P. D.; Howard, A. E.; Johnston, A. R.; Jordan, K. D. *J. Phys. Chem.* **1992**, *96*, 7570.
(15) Wei, Y.-H.; Cheng, H.-Y. *J. Phys. Chem.* **1998**.
(16) Binkley, J. S.; Pople, J. A.; Hehre, W. J. *J. Am. Chem. Soc.* **1980**, *102*, 939.
(17) Ditchfield, R.; Hehre, W. J.; Pople, J. *J. Chem. Phys.* **1971**, *54*, 724; Hehre, W. J.; Ditchfield, R.; Pople, J. A. *J. Chem. Phys.* **1972**, *56*, 2257; Hariharan, P. C.; Pople, J. A. *Theor. Chim. Acta* **1973**, *28*, 213.
(18) Paddon-Row, M. N.; Shephard, M. J.; Jordan, K. D. *J. Phys. Chem.* **1993**, *97*, 1743.
(19) Staley, S. W.; Strnad, J. T. *J. Phys. Chem.* **1994**, *98*, 116.
(20) Clark, T.; Chandrasekhar, J.; Spitznagel, G. W.; Schleyer, P. v. R. *J. Comput. Chem.* **1983**, *4*, 294; Hehre, W. J.; Ditchfield, R.; Pople, J. A. *J. Chem. Phys.* **1972**, *56*, 2257.
(21) Robin, M. B. *Higher Excited States of Polyatomic Molecules*; Academic Press: New York, 1974; Vol. 3.
(22) Robin, M. B. *Higher Excited States of Polyatomic Molecules*; Academic Press: New York, 1974; Vol. 1.
(23) Robin, M. B. *Higher Excited States of Polyatomic Molecules*; Academic Press: New York, 1974; Vol. 3, p 34.
(24) Mandelshtam, V. A.; Ravuri, T. R.; Taylor, H. S. *Phys. Rev. Lett.* **1993**, *70*, 1932.

(25) Malmqvist, P.-Å.; Rendell, A.; Roos, B. O. *J. Phys. Chem.* **1990**, *94*, 5477. Andersson, K.; Malmqvist, P.-Å.; Roos, B. O.; Sadlej, A. J.; Wolinski, K. *J. Phys. Chem.* **1990**, *94*, 5483.

(26) McLean, A. D.; Chandler, G. S. *J. Chem. Phys.* **1980**, *72*, 5639; Krishnan, R.; Binkley, J. S.; Seeger, R.; Pople, J. A. *J. Chem. Phys.* **1980**, *72*, 650; Clark, T.; Chandrasekhar, J.; Spitznagel, G. W.; Schleyer, P. v. R. *J. Comput. Chem.* **1983**, *4*, 294.

(27) The large number of configurations and roots stems from the fact that the programs can only albelian groups. Hence C_s symmetry was employed rather than D_{3d}.

(28) Frisch, M. J.; Trucks, G. W.; Schlegel, H. B.; Scuseria, G. E.; Robb, M. A.; Cheeseman, J. R.; Zakrzewski, V. G.; Montgomery, J. A.; Stratmann, R. E.; Burant, J. C.; Dapprich, S.; Millam, J. M.; Daniels, A. D.; Kudin, K. N.; Strain, M. C.; Farkas, O.; Tomasi, J.; Barone, V.; Cossi, M.; Cammi, R.; Mennucci, B.; Pomelli, C.; Adamo, C.; Clifford, S.; Ochterski, J.; Petersson, G. A.; Ayala, P. Y.; Cui, Q.; Morokuma, K.; Malick, D. K.; Rabuck, A. D.; Raghavachari, K.; Foresman, J. B.; Cioslowski, J.; Ortiz, J. V.; Stefanov, B. B.; Liu, G.; Liashenko, A.; Piskorz, P.; Komaromi, I.; Gomperts, R.; Martin, R. L.; Fox, D. J.; Keith, T.; Al-Laham, M. A.; Peng, C. Y.; Nanayakkara, A.; Gonzalez, C.; Challacombe, M.; Gill, P. M. W.; Johnson, B. G.; Chen, W.; Wong, M. W.; Andres, J. L.; Head-Gordon, M.; Replogle, E. S.; Pople, J. A. *Gaussian 98* (Revision A.7); Gaussian, Inc.: Pittsburgh, PA, 1998.

(29) Andersson, K.; Blomberg, M. R. A.; Fulscher, M. P.; Kello, V.; Lindh, R.; Malmqvist, P.-A.; Noga, J.; Olsen, J.; Roos, B. O.; Sadlej, A. J.; Siegbahn, P. E. M.; Urban, M.; Widmark, P.-O. MOLCAS, version 3; University of Lund, Sweden, 1994.

(30) Dunning, T. H., Jr. *J. Chem. Phys.* **1989**, *90*, 1007; Kendall, R. A.; Dunning, T. H., Jr.; Harrison, R. J. *J. Chem. Phys.* **1992**, *96*, 6769.

(31) Shimanouchi, T. *Tables of Molecular Vibrational Frequencies, Consolidated*; U.S. Govt. Printing Office: Washington, DC, Vol. 1 (NSRDS−NBS 39).

(32) Mulliken, R. S. *J. Chem. Phys.* **1955**, *23*, 1833.